Ionization by short uv laser pulses: Secondary above-threshold-ionization peaks of the electron spectrum investigated through a modified Coulomb-Volkov approach

V. D. Rodríguez,[1,2] E. Cormier,[1] and R. Gayet[1]
[1]*CELIA,* 1 Université Bordeaux 1, 351 Cours de la Libération, 33405 Talence Cedex, France*
[2]*Departamento de Física, FCEyN, Universidad de Buenos Aires, 1428 Buenos Aires, Argentina*
(Received 11 November 2003; revised manuscript received 13 January 2004; published 6 May 2004)

The interaction between an atom and a short laser pulse is studied in the case where both photon energies are smaller than the ionization potential and perturbation conditions prevail. Under these conditions, a full numerical solution of the time-dependent Schrödinger equation for a hydrogen atom initially in its ground state shows that secondary peaks show up in the above-threshold ionization (ATI) spectrum. We introduce here an easy-to-implement approximation that sheds light on these features. This approach, which is based on Coulomb-Volkov-type states, is an extension of a previous theory that applies only when photon energies are greater than the ionization potential. We show that introducing a coupling to intermediate bound states into the approach permits to nicely reproduce the full numerical electron spectrum for smaller photon energies. Further, it allows us to trace back unambiguously the secondary peaks to a manifold process, i.e., excitation of transient bound states followed by multiphoton absorption, and to show that the main ATI peaks may be enhanced by intermediate state contributions. When bound states with $1 \leqslant n \leqslant 4$ are included, the approach provides excellent predictions for photon energies as low as half the ionization potential.

DOI: 10.1103/PhysRevA.69.053402 PACS number(s): 42.50.Hz, 32.80.Rm, 32.80.Fb

I. INTRODUCTION

In recent works it was established that a simple theoretical approach, based on Coulomb-Volkov (CV) type states, can supply reliable predictions of atomic ionization by extreme ultraviolet laser pulses in the subfemtosecond regime [1,2]. For any field parameter, it was shown that the method provides accurate energy spectra of ejected electrons, including many above-threshold ionization (ATI) peaks, as long as the two following conditions are simultaneously fulfilled: (i) the photon energy is greater than or equal to the ionization potential; (ii) the ionization process is not saturated. Thus, ionization of atoms or molecules by the high-order harmonics (HOH) laser pulses which are currently generated [3] may be explored by this CV treatment which is called $CV2^-$ (this notation is used to distinguish it from CV1 that is another CV approach, based on the sudden approximation [4–6]). However, the condition (i) imposes a severe limitation on the application of $CV2^-$ to present-day HOH laser pulses. Reducing this limitation, while keeping the easiness of a CV treatment, is highly desirable to tackle ATI processes with smaller photon energies.

Indeed, trains of low-intensity laser pulses of a few hundreds of attoseconds have been produced in past years by harmonic generation techniques [3]. Such pulses are promising, powerful tools to investigate thoroughly the dynamics of subfemtosecond elementary processes (e.g., electronic evolution of microscopic systems) [7]. Both experiments and theories have shown that these techniques produce mainly odd harmonics whose intensity decreases very fast with the harmonics order, down to a well-known plateau. In the spectral region where a single photon can ionize a given atomic or molecular target, the intensity is several orders of magnitude smaller than the one of the fundamental frequency. Therefore, ATI processes produced by low-order harmonics of a given femtosecond pulse need special attention. Unfortunately, in the last decade, most theoretical approximations to ionization by laser beams were developed and implemented in a context of both much longer pulse durations and low photon energies (visible or infrared; see Ref. [2]). Yet, more adapted close-coupling calculations were recently performed by Kondorskiy and Presnyakov [9]. They showed that the electron spectrum resulting from the ionization of H(1*s*) atoms by 3.8 eV photons of a 14 fs linearly polarized laser pulse with a fairly high intensity is deeply affected by the influence of bound intermediate states. Including the states $n=2$ in their calculations results in a global increase of the energy electron distribution and, more interestingly, in the appearance of new structures in the spectrum. In the present paper, we first perform full numerical studies of the time-dependent Schrödinger equation using the code written by Cormier that implements a full three-dimensional (3D) numerical approach. It is based on a *B*-spline basis set expansion [8]. Predictions of this approach, hereafter referred to as TDSE, may be regarded as "exact" ones [8]. In the simplest case of a hydrogen atom H(1*s*) interacting with a short laser pulse whose photon energy is smaller than the ionization potential, TDSE predicts that secondary peaks show up in the ATI spectrum, besides the sequence of main ATI peaks. Calculations have been carried out in perturbation conditions, thus avoiding peak shift due to the ponderomotive energy [1]. It will be shown that it is the right situation that allows us to trace back the new structures to transient formation of bound states with subsequent multiphoton absorption.

However, full numerical treatments involve intensive calculations [8] that sometimes may obscure the essential phys-

*Centre Lasers Intenses et Applications (UMR 5107, Unité Mixte de Recherche CNRS Université Bordeaux 1); http://www.celia.u-bordeaux.fr

 ©2004 The American Physical Society

ics of the problem. Further, addressing two-electron systems with TDSE appears much more involved. Therefore, the analysis of future experiments calls for adapted theoretical approximations that are able to provide simple reliable predictions of ionization by short uv laser pulses. In this context, the CV2$^-$ approach is reexamined here. We introduce a modified form of CV2$^-$ that aims at accounting for the features that the above-mentioned TDSE calculations reveal in the electron spectrum when the photon energy is below the ionization potential. In what follows, as in Ref. [1], TDSE predictions are used to delimit the domain where the present extension of the approach CV2$^-$, hereafter referred to as MCV2$^-$, applies. Again, any further complication is avoided by considering the reference example of the ionization of a hydrogen atom initially in its ground state. Just as CV2$^-$, MCV2$^-$ is a perturbation approach. Indeed, making the study in perturbation conditions permits us to concentrate on the influence of the photon frequency. Further, improvements and failures of the standard CV2$^-$ may be evidenced more easily.

In Sec. II, the CV2$^-$ theory is briefly reviewed in the context of short xuv laser pulses. The MCV2$^-$ theory (modified CV2$^-$) is derived using a variational principle for the transition amplitude [10]. It is proposed after examining important failures of CV2$^-$ in the prediction of ionization spectra with photon energies smaller than the ionization potential.

In Sec. III, MCV2$^-$ is applied in situations connected to present-day HOH radiations. Conditions where TDSE predictions are well reproduced by MCV2$^-$ are illustrated for spectra of electrons ejected from H(1s) atoms. Further, comparing predictions of CV2$^-$, MCV2$^-$, and TDSE enables us to confirm without a doubt that the new structures showing up in the electron spectrum are due to multiphoton absorption from transitory excited bound states. The influence of both the laser duration and the photon energy are also studied in detail. Conclusions are drawn in Sec. IV. Atomic units are used throughout unless otherwise stated.

II. THEORY

We consider here the ionization of a one-active electron atom by an external laser radiation whose electric field is $\vec{F}(\vec{r},t)$. Under nonrelativistic conditions and within the electric dipole approximation the electron wave function $\Psi(\vec{r},t)$ satisfies the time-dependent Schrödinger equation

$$i\frac{\partial \Psi(\vec{r},t)}{\partial t} = [H_a + \vec{r}\cdot\vec{F}(t)]\Psi(\vec{r},t),$$

$$H_a = -\frac{\nabla^2}{2} + V_a(\vec{r}), \tag{1}$$

where $\vec{r}$ is the position of the electron with respect to the nucleus identified with the center of mass, $\vec{F}(t)$ is the laser field in the volume of the atom, and $V_a(\vec{r})$ is the interaction between the electron and the rest of the target. In the ionization process, the initial bound state $\phi_i(\vec{r},t)$ and the final continuum state $\phi_f^-(\vec{r},t)$ may be written as

$$\phi_i(\vec{r},t) = \varphi_i(\vec{r})\exp(-i\varepsilon_i t),$$

$$\phi_f^-(\vec{r},t) = \varphi_f^-(\vec{r})\exp(-i\varepsilon_f t), \tag{2}$$

where $\varphi_i(\vec{r})$ and $\varphi_f^-(\vec{r})$ are eigenstates of the field-free Hamiltonian H_a and $\varphi_f^-(\vec{r})$ is the ingoing continuum state of momentum $\vec{k}$ normalized to $\delta(\vec{k}-\vec{k}')$. In the present work we focus on the hydrogen atom although the formalism remains valid for any one-active electron system where a reasonable model or pseudopotential $V_a(\vec{r})$ may be used to represent the interaction of the active electron with the rest of the system.

The finite pulse duration is featured by a sine-square envelope. Thus, in the vicinity of the atom the external electric field reads

$$\vec{F}(t) = \begin{cases} \vec{F}_0\sin(\omega t+\varphi)\sin^2\left(\dfrac{\pi t}{\tau}\right) & \text{when } t\in[0,\tau] \\ \vec{0} & \text{elsewhere}, \end{cases} \tag{3}$$

where τ is the total duration of the pulse. The laser electric field is derived from a vector potential $\vec{A}(t)$ which may be written as

$$\vec{A}(t) = \vec{A}(t_0) - \int_{t_0}^{t} dt'\vec{F}(t'). \tag{4}$$

In the Schrödinger picture, the transition amplitude from the state i at $t=0$ to the final state f at $t=\tau$ may be approximated by the *prior* form of the following variational expression [10]:

$$a_{fi}^- = \lim_{t\to 0}\langle\chi_f^-(t)|\chi_i^+(t)\rangle - i\int_0^\tau dt\langle\chi_f^-(t)|\overleftarrow{H - i\frac{\partial}{\partial t}}|\chi_i^+(t)\rangle, \tag{5}$$

where the arrow on the left-hand side indicates the state on which the non-Hermitian operator applies; $\chi_f^-(\vec{r},t)$ and $\chi_i^+(\vec{r},t)$ are trial functions to the exact solutions of Eq. (1), subject to the asymptotic conditions

$$\chi_f^-(\vec{r},t) \underset{t\to\tau}{\sim} \phi_f^-(\vec{r},t), \tag{6a}$$

$$\chi_i^+(\vec{r},t) \underset{t\to 0}{\sim} \phi_i(\vec{r},t). \tag{6b}$$

Expression (5) provides exact transition amplitudes when one of the two trial functions are exact solutions of Eq. (1). The Coulomb-Volkov wave function [1,2] is used as the trial wave function $\chi_f^-(\vec{r},t)$:

$$\chi_f^-(\vec{r},t) = \phi_f^-(\vec{r},t)L^-(\vec{r},t) \tag{7}$$

$$L^-(\vec{r},t) = \exp\left\{i\vec{A}^-(t)\cdot\vec{r} - i\vec{k}\cdot\int_\tau^t dt'\vec{A}^-(t') - \frac{i}{2}\int_\tau^t dt'\vec{A}^{-2}(t')\right\},$$

where $\vec{A}^-(t)$ is the variation of $\vec{A}(t)$ over the time interval $[\tau,t]$, i.e.,

$$\vec{A}^{-}(t) = -\int_{\tau}^{t} \vec{F}(t)dt. \tag{8}$$

After an easy algebra using Eqs. (7) and (8), the expression (5) may be transformed into

$$a_{fi}^{-} = \int_{0}^{\tau} dt \exp\left\{ i\frac{k^2}{2}t + i\vec{k}\cdot\int_{\tau}^{t} dt'\vec{A}^{-}(t') + \frac{i}{2}\int_{\tau}^{t} dt'\vec{A}^{-2}(t') \right\}$$
$$\times \int d\vec{r}\chi_i^{+}(\vec{r},t)\exp[-i\vec{A}^{-}(t)\cdot\vec{r}]\vec{A}^{-}(t)\cdot[i\vec{k}+\vec{\nabla}]\varphi_f^{-*}(\vec{r}). \tag{9}$$

For a realistic laser pulse, the first term in Eq. (5) is zero because both $\vec{A}^{-}(0)=\vec{0}$ (no direct electric field) and $\phi_i(\vec{r},t)$ and $\phi_f^{-}(\vec{r},t)$ are orthogonal. But the choice of the trial wave function $\chi_i^{+}(\vec{r},t)$ in expression (9) is still open. In fact the so-called CV2^{-} approximation is obtained from Eq. (9) by replacing $\chi_i^{+}(\vec{r},t)$ by the unperturbed wave function $\phi_i(\vec{r},t)$. Then, the CV2^{-} transition amplitude may be written as

$$a_{fi}^{CV2-} = \int_{0}^{\tau} dt \exp\left\{ i\left(\frac{k^2}{2}-\varepsilon_i\right)t + i\vec{k}\cdot\int_{\tau}^{t} dt'\ \vec{A}^{-}(t') + \frac{i}{2}\int_{\tau}^{t} dt'\ \vec{A}^{-2}(t') \right\}\int d\vec{r}\varphi_i(\vec{r})$$
$$\times\exp[-i\vec{A}^{-}(t)\cdot\vec{r}]\ \vec{A}^{-}(t)\cdot[i\vec{k}+\vec{\nabla}]\ \varphi_f^{-*}(\vec{r}). \tag{10}$$

The integration over the electron coordinate may be expressed in terms of the well-known bound-continuum form factor. For hydrogen atoms, it is analytical using Nordsieck's integrals [11]. Therefore, just a simple time numerical integration over the pulse length is necessary to evaluate a_{fi}^{CV2-}. Then, as usual, the angular distribution of ejected electrons is given by

$$\frac{\partial^2 P_{fi}}{\partial E_K\,\partial\Omega_k} = k|a_{fi}^{-}|^2, \tag{11}$$

where E_k and Ω_k are the energy of the ejected electron and the direction of its impulse $\vec{k}$, respectively. Integrating over Ω_k provides the energy distribution $\partial P_{fi}/\partial E_K$. A further integration over E_k yields the total ionization probability P_{ion}.

Previous studies [1] have shown that the CV2^{-} approach (10) leads to accurate energy spectra of ejected electrons, including all the ATI peaks, provided that both the photon energy is greater than or equal to the ionization potential and the ionization process is not saturated. In fact, the second condition means that the ionization probability should not exceed 20–30 %. In this work, we propose to improve the CV2^{-} theory in order to get rid of the first limitation. However, the basis of the CV2^{-} approach requires that perturbation conditions be preserved. In practice, it is not a limitation. Moreover, keeping perturbation conditions permits us to track more easily the other causes of failure of the standard CV2^{-}.

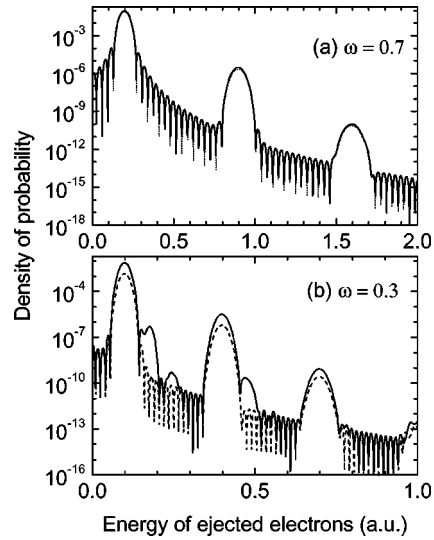

FIG. 1. Ionization of H(1s): distribution of ejected electrons (density of probability per energy range) as a function of the electron energy for a laser field amplitude $F_0=0.01$ and two pulse durations, each corresponding to 20 cycles. The photon energy is $\omega=0.7$ ($\tau=179.52$) (a) and $\omega=0.3$ ($\tau\simeq 419$ a.u.$\simeq 10$ fs) in (b). Dashed line, CV2^{-}; full line, TDSE. All quantities are given in atomic units.

Electron energy spectra as predicted by CV2^{-} and TDSE are reported in Fig. 1 for photon energies above and below the ionization potential $|\varepsilon_i|=0.5$. It is worth noting that an accurate and fast numerical time integration method has been implemented. Thus, the round-off errors identified in Ref. [1] have now been corrected [13]. To ensure perturbation conditions, the laser field is set to $F_0=0.01$ ($I\approx 3.5\times 10^{12}$ W cm^{-2}). For $\omega=0.7$, there is an excellent agreement between the two spectra [Fig. 1(a)]. The height and the position of the peaks are very well reproduced by CV2^{-}. On the contrary, significant differences show up for $\omega=0.3$ [Fig. 1(b)]: all ATI peaks predicted by CV2^{-} are smaller than TDSE ones, while TDSE let appear a new set of secondary peaks that are unexplained by the standard CV2^{-} theory. In fact, due to energy conservation, the main ATI peaks are found at the following energies:

$$E_p = \varepsilon_i + p\omega, \tag{12}$$

where p is the number of absorbed photons. In the present case, the ponderomotive energy $U_p=F_0^2/4\omega^2$ is negligible because of both the low laser intensity and the high photon frequency. Further, one may notice that the secondary peak position follows a similar rule:

$$E_{s,n} = \varepsilon_n + s\omega, \tag{13}$$

where $s>0$ and $n>1$ are integers. Thus, it suggests that the secondary peaks may be traced back to the absorption of s photon(s) from excited states $n=2,3\ldots$. The occurrence of secondary structures has been extensively studied in ATI in the context of strong-field experiments [14,15]. The substructures observed in ATI spectra that are produced in these experiments are due to the system shifting into resonances as

the intensity increases, thus giving rise to an enhancement of the production of electrons at energies related to the actual binding energies of the Rydberg states in the external laser field. It is worth noting that our observations have a fundamentally different origin. In our case, the resonances get population even far detuned only because the field has a broadband spectrum while the intensity is too low to induce any ponderomotive shift.

For instance, the background in Fig. 1(a) is fully explained by the first Born approximation, while subsequent photon absorptions require Born terms of higher order. Hence, improving the CV2$^-$ theory implies taking into account a pathway through intermediate bound states. A simple way to do it consists in a different choice for the trial wave function $\chi_i^+(\vec{r},t)$. Since the first Born approximation reproduces very well the nonresonant background of the whole spectrum, even very far from the ionization threshold, it is natural to propose the following form for $\chi_i^+(\vec{r},t)$:

$$\chi_i^+(\vec{r},t) = \sum_j a_{ji}^{B1}(t)\phi_j(\vec{r},t), \tag{14}$$

where $a_{ji}^{B1}(t)$ is the first Born approximation transition amplitude at time t from the initial state i to the intermediate state $j \equiv (n,l,m)$. In principle, the sum runs on all the atomic states $\phi_j(\vec{r},t)$. However, $a_{ji}^{B1}(t)$ reads

$$a_{ji}^{B1}(t) = -i\int_0^t \exp\{i(\varepsilon_j - \varepsilon_i)t'\}\vec{F}(t')dt' \cdot \int d\vec{r}\varphi_j^*(\vec{r})\vec{r}\varphi_i(\vec{r}). \tag{15}$$

Therefore, $a_{ji}^{B1}(t)$ is zero if the intermediate state j does not satisfy the appropriate electric dipole selection rules. If the laser field is linearly polarized in the z direction and if the initial state i is the ground state $1s$, these rules impose $l=1$ and $m=0$. In this case, the trial wave function may be written as

$$\chi_i^+(\vec{r},t) = \phi_i(\vec{r},t) + \sum_{n>1}^{N} a_{np0,1s}^{B1}(t)\phi_{np0}(\vec{r},t), \tag{16}$$

where N is the maximum principal quantum number that is kept in the summation. In principle, the expression of $\chi_i^+(\vec{r},t)$ in Eq. (16) should be renormalized. In fact, due to the very small absolute values of all amplitudes $a_{np0,1s}^{B1}(t)$, it appears unnecessary to do so in the subsequent applications. Thus, the transition amplitude for the present theory takes the form

$$\begin{aligned} a_{fi}^{MCV2-} = a_{fi}^{CV2-} + \sum_{n>1}^{N}\int_0^\tau dt\; b_{ji}^{B1}(t)\exp\Bigg\{ & i\left(\frac{k^2}{2} - \varepsilon_j\right)t \\ & + i\vec{k}\cdot\int_\tau^t dt'\; \vec{A}^-(t') \\ & + \frac{i}{2}\int_\tau^t dt'\; \vec{A}^{-2}(t')\Bigg\}\vec{A}^-(t)\cdot\int d\vec{r}\varphi_j(\vec{r}) \\ & \times\exp[-i\,\vec{A}^-(t)\cdot\vec{r}]\;\vec{A}^-(t)\cdot[i\vec{k}+\vec{\nabla}]\;\varphi_f^{-*}(\vec{r}), \end{aligned} \tag{17}$$

where n stands now for the principal quantum number of an intermediate state $j=(n,p,0)$. We observe that the first term accounts for the usual ATI peaks as given by the standard CV2$^-$ theory (10), while the second term represents a series of CV2$^-$ amplitudes for transitions starting from intermediate states j. These amplitudes are weighted by the first Born transition amplitude (15) at any time during the laser pulse. Their meaning is quite simple: to undergo a transition into a continuum state, the system can first be excited into an upper bound state through a single-photon absorption, then undergo a final multiphoton transition into the final state. The first step, which is described by the first Born transition amplitude, is possible, even in nonresonant situations, because the finite duration of the pulse results in a broadening of the laser frequency. By the way, it is worth noting that the present procedure works in both resonant and nonresonant conditions in the first step, thus avoiding the difficulties linked with poles that appear in higher orders of the Born series.

Now, each amplitude of the second term in Eq. (17) reaches its maximum value when the integrant is as slowly oscillating as possible. In the expression (17) of $a_{fi}^{MCV2^-}$, the most rapidly oscillating factor in the time integration is $\exp\{i(k^2/2-\varepsilon_j)t\}\vec{A}^-(t)$. Its oscillation is removed when $k^2/2-\varepsilon_j$ corresponds to the energy of p photons. Thus, when the first step is a nonresonant process, i.e., when $\varepsilon_j-\varepsilon_i-\omega\neq 0$ in the expression (15), one expects to see secondary peaks showing up besides the principal peaks for values of k such that $k^2/2-\varepsilon_j-p\omega=0$. Indeed, the principal peaks are direct transitions corresponding to $k^2/2-\varepsilon_i-p'\omega=0$. They are the only ones to be accounted for in $a_{fi}^{CV2^-}$.

Further, when the first step is a nonresonant process, the expression (15) indicates that the closer to zero the value of $\varepsilon_j-\varepsilon_i-\omega$, the higher is the contribution of $a_{ji}^{B1}(t)$ to the amplitude of the secondary peak related to the intermediate state j. Therefore, the height of a secondary peak increases when the associated intermediate state j gets close to resonance. But at the same time, the secondary peak gets closer to a principal peak which results in interferences between the two amplitudes. Thus, heights and shapes of the two peaks may be affected when they are very close to each other. One gets a good indication on the influence of interferences by comparing standard CV2$^-$ and MCV2$^-$ predictions.

In the case of an exact resonance, i.e., when $\varepsilon_j-\varepsilon_i-\omega=0$ for a given intermediate state j, the two (direct and indirect) quantum pathways cannot be distinguished. Again the role played by the intermediate state is proved by comparing CV2$^-$ and MCV2$^-$ predictions.

In the subsequent applications, we have checked that the convergence is achieved in Eq. (17) for $N<4$. In fact, secondary peaks for higher intermediate states vanish in the background.

III. APPLICATION OF MCV2$^-$ TO THE IONIZATION OF HYDROGEN ATOMS

In order to investigate to which extent the present MCV2$^-$ applies, we address here the ionization of hydrogen atoms in

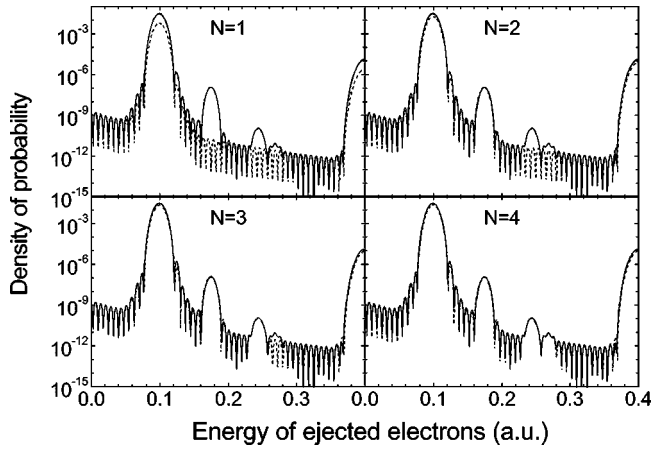

FIG. 2. Ionization of H(1*s*): distributions of ejected electrons as functions of the electron energy for different values of the maximum quantum number N of intermediate states [see text, Eq. (17)]. The laser parameters are field amplitude $F_0=0.01$, photon energy $\omega=0.3$, and a 40 cycle pulse ($\tau\simeq 838$ a.u.$\simeq 20$ fs). Dotted line, MCV2$^-$; full line, TDSE. All quantities are given in atomic units.

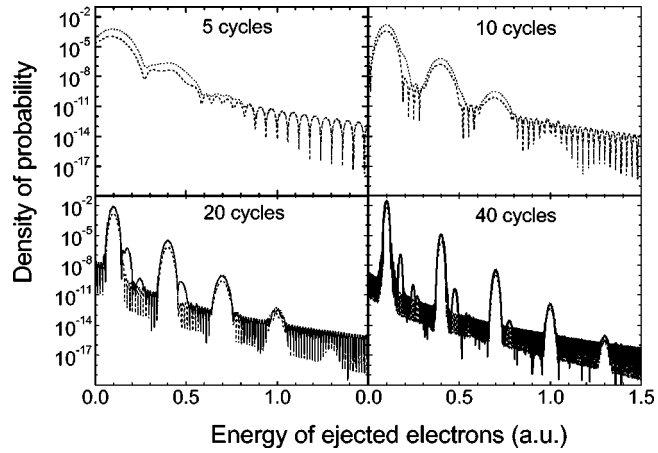

FIG. 3. Ionization of H(1*s*): distributions of ejected electrons as functions of the electron energy for different pulse durations. The other laser parameters are field amplitude $F_0=0.01$ and photon energy $\omega=0.3$. Dashed line, CV2$^-$; dotted line, MCV2$^-$; full line, TDSE (only displayed for 20 and 40 cycles). All quantities are given in atomic units.

their ground state by a laser pulse whose photon energy is smaller than the ionization potential. As already mentioned, we restrict our investigations to the perturbation regime by fixing the laser field amplitude at $F_0=0.01$. First, we analyze the convergence of the summation in Eq. (17). We show that successive secondary peaks appear when one raises N, i.e., when more intermediate states are incorporated. We also show that one reaches rapidly a maximum value of N where additional secondary peaks merge in the background. Then, the issue of pulse duration dependence is highlighted. Finally, different photon energies are considered, ranging from 0.25 (not even able to excite the first excited state) to almost the ionization potential.

A. Convergence on the intermediate state summation

We run the test for the following parameters of the laser pulse: a frequency $\omega=0.3$ and a pulse duration $\tau=837.7$ a.u. ($\simeq 20.3$ fs) corresponding to 40 cycles. So, it is comparable to the pulse length of a *given* high harmonics [12]. It allows us to get well separated ATI peaks. Further, the value of ω does not permit to ionize H(1*s*) with the absorption of a single photon. Therefore, the first ionization peak located close to $\varepsilon_f=0.1$ corresponds to a two-photon process. In Fig. 2, electron energy spectra predicted by MCV2$^-$ are compared to TDSE spectra for increasing value of the parameter N. The electron energy range is limited to clearly show the first set of secondary peaks. Thus, only the first two principal peaks are displayed here. They are located at $\varepsilon_f=0.1$ and $\varepsilon_f=0.4$ a.u., respectively. Since a single-photon absorption does not permit to reach the first excited level, the secondary peaks associated with intermediate bound-state excitation followed by one-photon absorption should lie close to $\varepsilon_f=\varepsilon_j+\omega$, i.e., in between the first and the second primary peaks. It is noteworthy that MCV2$^-$ reproduces the standard CV2$^-$ predictions with $N=1$ in Eq. (17). In this case, one sees that both the main peaks are underestimated and no secondary peak shows up. For $N=2$, the main peaks as predicted by MCV2$^-$ are enhanced and the first secondary peak as predicted by TDSE is well reproduced by MCV2$^-$. Therefore, contribution to the first secondary peaks may be entirely traced back to the intermediate level $n=2$. In the case $N=3$, the convergence for height and shape of the main peaks is almost achieved while the secondary peak corresponding to the excited level $n=3$ also shows up.

Finally, for $N=4$, the whole spectrum is fully recovered. The agreement between MCV2$^-$ and TDSE is almost perfect. The influence of higher intermediate states is negligible since their excitation amplitude vanishes rapidly when one increases the principal quantum number. Thus, the contributions to the electron spectrum from all intermediate states with $n>4$ are wiped out by the overwhelming contribution of the background.

B. Influence of the pulse duration

In Fig. 3, electron spectra corresponding to various laser pulse durations τ are displayed. Calculations are performed for $\omega=0.3$ and for τ ranging from 5 to 40 cycles (2.5 fs $\leqslant\tau\leqslant$ 20.3 fs). The number of observable ATI peaks increases with τ. Indeed, the background, which is given by the first Born approximation, behaves as the Fourier transform of $F(t)$, while the height of ATI peaks grows as τ^2 and their width shrinks as $1/\tau$. As a result, the probability integrated over any principal ATI peak follows the well-known linear dependence on τ, which simply means that the multiphoton ionization rate becomes constant when τ is large enough.

Now, when τ increases, the height of the two-step secondary peaks decreases because the nonresonant first step occurs on a wing of a one-photon absorption peak as given by the first Born approximation. Since the second step is a resonant multiphoton transition from an intermediate level, its probability varies like τ^2. Thus, the overall height of secondary peaks increases with respect to the background, although it

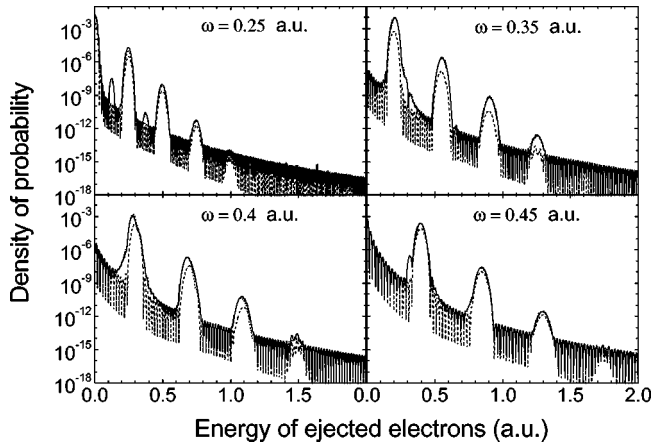

FIG. 4. Ionization of H(1*s*): distributions of ejected electrons as functions of the electron energy for different photon energies. The other laser parameters are field amplitude $F_0=0.01$ and pulse durations corresponding to 20 cycles. Dashed line, CV2$^-$; dotted line, MCV2$^-$; full line, TDSE. All quantities are given in atomic units.

decreases in absolute value. As the width of secondary peaks follows the standard $1/\tau$ behavior, we conclude that the integrated probability over a secondary peak vanishes for long pulse durations. Nevertheless, when the pulse duration increases, the secondary peaks are better resolved because both their width is reduced and the background decreases faster than their height. In the present application with a sine-square envelope of the laser pulse, it is easy to show that the background decreases as τ^{-4} [13]. No matter what the envelope is, nonresonant secondary peaks will show up only when atomic ionization is made by short, *but not too short*, laser pulses.

From the comparison between CV2$^-$ and MCV2$^-$, we also observe noticeable discrepancies in the height of the main ATI peaks. These differences are visible even for the shortest pulse duration (5 cycles). Thus, MCV2$^-$ not only reproduces the secondary peaks and explains their origin, but it also improves magnitude and shape of the principal ATI peaks with respect to the predictions made by CV2$^-$. As it is explained above, these changes follow from the form (17) of $a_{fi}^{MCV2^-}$. The transition amplitude for a principal peak can interfere noticeably with the amplitude of a secondary peak close to it. One sees that the outcome is to always increase the height of the principal peak, thus showing constructive interferences.

Finally, it is worth noting that the period of the oscillations, which appear clearly beyond 0.8 a.u. in all spectra of Fig. 3, is exactly $2\pi/\tau$. It is no wonder since it corresponds to the Fourier transform of the envelope, which oscillates one time with a period τ in the present application.

C. Influence of the photon energy

So far, we have examined atomic ionization by a laser pulse for a given photon energy. Let us now consider a pulse composed of 20 cycles with different values of ω. To remain clearly in the perturbation regime, we keep the same laser intensity, i.e., $F_0=0.01$. In Fig. 4, we compare the electron spectra given by CV2$^-$, MCV2$^-$, and TDSE for four values of $P_{fi}^{CV2^-}$, $P_{fi}^{MCV2^-}$, and P_{fi}^{TDSE} for four values of ω below the ionization potential ($0.35\leqslant\omega\leqslant 0.45$). It is worth noting that, down to $\omega=0.35$, there is a perfect agreement between MCV2$^-$ and TDSE. As expected, CV2$^-$ does not agree with the latter. Further, secondary peaks appear as shoulders of principal peaks when they are not well resolved.

Now, for $\omega=0.25$, both MCV2$^-$ and CV2$^-$ underestimate the height of the principal peaks as given by TDSE. However, MCV2$^-$ appears much better than CV2$^-$ and the two secondary peaks which show up above the background are well reproduced by MCV2$^-$. The first and second secondary peaks are the signature of one- and two-photon absorption from the excited state $n=2$, respectively. Since the bound energy of the state $n=2$ is -0.125, i.e., half the value of ω, the secondary peaks stand out above the background at equal distances of the neighboring principal peaks. As to the small discrepancy between the heights of MCV2$^-$ and TDSE principal peaks, it might be traced back to the contribution from intermediate Rydberg states that are almost at resonance of a two-photon absorption for $\omega=0.25$. Indeed, such a contribution is not taken into account in the present model because the coefficients $b_{ji}^{B1}(t)$ in Eq. (17) are first Born approximation amplitudes that can only describe one-photon absorption. Further, we have shown that the convergence of the summation over intermediate levels for a one-photon absorption is achieved for $n=4$. Therefore, including more Rydberg states would be useful only if multiphoton absorption to intermediate levels could be made. Since it is not possible in the present approach MCV2$^-$, one may assess its lower limit of application to $\omega=0.25$.

Finally, the analysis of the positions of secondary peaks for the different values of ω confirms that their origin is the above-mentioned two-step process. For $\omega=0.35$, the first secondary peak due to the level $n=2$ is a shoulder on the right wing of the first principal peak (direct two-photon absorption). Further, two secondary peaks, traced back to a one- and two-photon absorption from the intermediate level $n=3$, loom up at the expected place to the right of the first and second principal peaks, respectively. For $\omega=0.45$, the only resolved secondary peak is located to the left of the first principal peak at a place that permits us to ascribe it to the intermediate level $n=2$. It appears also as a shoulder in the left wing of the second principal peak.

Scrutinizing the case $\omega=0.40$ reveals that the first secondary peak is larger than the first principal peak. It is attested by both its position, and the position and height of the principal peak as predicted by CV2$^-$. Thus, the first principal peak manifests itself as a shoulder in the right wing of the secondary peak. Actually, the energy separation between the two peaks is 0.05 a.u. Indeed, this case corresponds to an almost resonance situation (which would occur for $\omega=0.375$ a.u.). Further, the shape of the first peak lets appear a large width, especially visible on the left wing. The shape is characteristic of a single-photon ionization as given by the first Born approximation [see Fig. 1(b)]. It is without doubt the signature of the first step leading to a secondary peak (here, the excitation of the intermediate level $n=2$).

To support this statement, we display, in Fig. 5, spectra that are obtained for the resonant case, i.e., $\omega=0.375$ a.u..

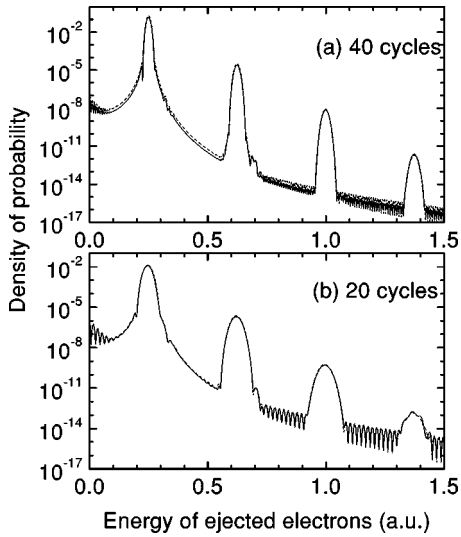

FIG. 5. Ionization of H(1*s*): distributions of ejected electrons as functions of the electron energy for a photon energy $\omega=0.375$ corresponding to the excitation energy of H(2*p*). The other laser parameters are field amplitude $F_0=0.01$ and pulse durations corresponding to (a) 40 cycles and (b) 20 cycles. Dashed line, MCV2$^-$; full line, TDSE. All quantities are given in atomic units.

Two pulse durations are considered: (a) 40 cycles and (b) 20 cycles. In the full spectrum there is still an overall good agreement between MCV2$^-$ and TDSE simulations. In Fig. 6, we focus on the two first ionization peaks. We observe again the typical form of a first Born approximation maximum. However, slight differences show up: MCV2$^-$ is above TDSE for the long pulse while it remains close to TDSE for the short pulse. The explanation is simple: at the resonance between the fundamental photon energy and the excitation energy of a given intermediate state, the first Born approximation probability increases as the square of the pulse duration. Therefore, one expects that it will overestimate the actual transition probability as the pulse duration increases. However, it is interesting to see that it remains acceptable for pulse durations corresponding to the length of a single pulse in a train of attosecond laser pulses produced by harmonic generation techniques [3].

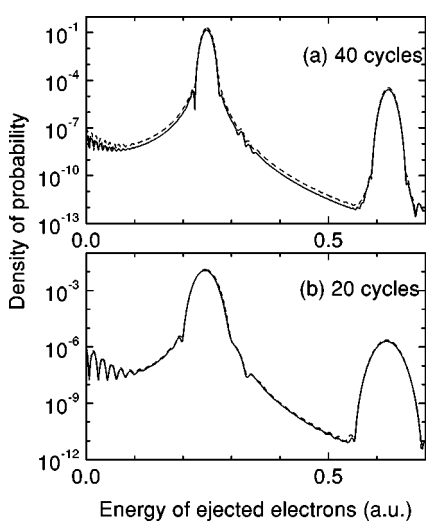

FIG. 6. Same as Fig. 5 but with a close-up on the first two ionization peaks.

Now, it is worth noting that, contrary to the usual resolvent method, the approach MCV2$^-$ does not deal with poles. Therefore, resonant and nonresonant intermediate states are treated on an equal footing. The procedure works as long as perturbation conditions prevail.

IV. CONCLUSIONS AND OUTLOOK

We have shown that substituting the genuine initial state for a new *bound* state, which corresponds to an evolution of the initial state under the influence of the laser field, permits to reproduce accurately the ionization process for photon energies smaller than the ionization potential. The new bound state takes into account the possibility to form transient intermediate bound states all along the laser pulse, thus allowing the multiphoton ionization process to occur from these intermediate levels. In the present MCV2$^-$ theory, the new initial state is made of the genuine initial state plus a limited number of bound intermediate states, whose coefficients are given, with the correct phase, by the amplitude of the first Born approximation. Therefore, only levels that may be reached through a one-photon transition appear in the expansion. As a result, one expects MCV2$^-$ to apply as long as multiphoton transitions are negligible in the formation of upper bound states. Thus, we may conclude that MCV2$^-$ applies when the photon energy is higher than, say, half the ionization potential of the target.

Therefore, if one wants to investigate the ionization by laser pulses with softer photon energies by means of a similar Coulomb-Volkov approach, it appears necessary to take into account multiphoton processes in the formation of intermediate states. It might be achieved by replacing, in the expansion (16), the amplitudes of the first Born approximation by the more adapted time-dependent Coulomb-Volkov amplitudes CV2$^+$ as defined in Ref. [2].

Finally, it is worth noting that MCV2$^-$ is very simple to implement, not only in the simplest case of hydrogen atoms. The aim of present studies is to evaluate the domain where MCV2$^-$ is applicable. Within this domain, application to ionization of complex atoms is straightforward if bound wave functions may be obtained in the form of Slater-type orbital expansions. More precisely, double photoionization by short uv laser pulses may be envisaged in the framework of two-active electron. Preliminary promising calculations have been made for double ionization of helium by synchrotron radiation [16]. Further, application to ionization of diatomic molecules is also envisaged. Let us indicate also that addressing different types of laser fields is made easy with a Coulomb-Volkov approach in the length gauge because all field parameters are contained in the vector potential $\vec{A}(t)$. Therefore, photons may have linear, elliptic, or circular polarizations, two-color transitions (with coherent or noncoherent beams) may be studied, etc. Thus, as long as perturbation conditions are achieved, Coulomb-Volkov approaches open a wide range of applications to short laser pulse interactions.

ACKNOWLEDGMENTS

V.D.R. acknowledges support by the Universidad de Buenos Aires and the Agencia Nacional de Promoción Científica y Tecnológica (Contrato de Préstamo BID Contract No. 802 OC-AR, Grant Nos. 03-04021 and 03-06249). He also acknowledges a one-month position as Invited Professor given by the Université Bordeaux 1 to prolong his stay at the Centre Laser Intenses et Applications. The calculations were performed within the new M3PEC pole for parallel computing at the Université Bordeaux 1.

[1] G. Duchateau, E. Cormier, and R. Gayet, Phys. Rev. A **66**, 023412 (2002).
[2] G. Duchateau, E. Cormier, H. Bachau, and R. Gayet, J. Mod. Opt. **50**, 331 (2003).
[3] P. M. Paul, E. S. Toma, P. Breger, G. Mullot, F. Augé, Ph. Balcou, H. G. Muller, and P. Agostini, Science **292**, 1689 (2001).
[4] G. Duchateau, E. Cormier, and R. Gayet, Eur. Phys. J. D **11**, 191 (2000).
[5] G. Duchateau, C. Illescas, B. Pons, E. Cormier, and R. Gayet, J. Phys. B **33**, L571 (2000).
[6] G. Duchateau, E. Cormier, H. Bachau, and R. Gayet, Phys. Rev. A **63**, 053411 (2001).
[7] M. Drescher *et al.*, Nature (London) **419**, 803 (2002).
[8] E. Cormier and P. Lambropoulos, J. Phys. B **30**, 77 (1997).
[9] A. D. Kondorskiy and L. P. Presnyakov, J. Phys. B **34**, L663 (2001).
[10] Yu N. Demkov, *Variational Principles in the Theory of Collisions* (Pergamon Press, Oxford, 1963).
[11] A. Nordsieck, Phys. Rev. **93**, 785 (1954).
[12] A. Bouhal, P. Salières, P. Breger, P. Agostini, G. Hamoniaux, A. Mysyrowicz, A. Antonetti, R. Constantinescu, and H. G. Muller, Phys. Rev. A **58**, 389 (1998).
[13] V. D. Rodríguez and R. Gayet (unpublished).
[14] R. R. Freeman, P. H. Bucksbaum, H. Milchberg, S. Darack, D. Schumacher, and M. E. Geusic, Phys. Rev. Lett. **59**, 1092 (1987); for a recent reference, see G. D. Gillen and L. D. Van Woerkom, Phys. Rev. A **68**, 033401 (2003).
[15] M. P. de Boer and H. G. Muller, Phys. Rev. Lett. **68**, 2747 (1992).
[16] G. Duchateau, Ph.D. thesis, Université Bordeaux 1, 2001 (unpublished).